

# The Anderson prescription for surfaces and impurities

K. Tanaka and F. Marsiglio

*Department of Physics, University of Alberta, Edmonton, Alberta, Canada T6G 2J1*

(February 5, 2020)

We test the Anderson prescription [1], a BCS formalism for describing superconductivity in inhomogeneous systems, and compare results with those obtained from the Bogoliubov-de Gennes formalism, using the attractive Hubbard model with surfaces and nonmagnetic impurities. The Anderson approach captures the essential features of the spatial variation of the gap parameter and electron density around a surface or an impurity over a wide range of parameters. It breaks down, however, in the strong-coupling regime for a weak impurity potential.

In microscopic treatments of inhomogeneity effects in superconductors, impurities are often averaged over in some manner [1,2]. In the last decade, partly because of the increased computational resources now available, and partly because of the technical advances which allow small particle fabrication and single atom manipulation [3], the role of inhomogeneous effects in superconductors has received more wide-spread attention [4]. One of the theoretical frameworks for addressing these questions is the Bogoliubov-de Gennes (BdG) formalism [5]. This formalism allows one to answer questions regarding surfaces, interfaces, and impurity effects at a level of detail not previously addressed. At present, however, the scope of problems for which one can compute results accurately is limited by computer resources, since matrices whose dimension grows with system size require full diagonalization and should be solved self-consistently. On the other hand, the Anderson prescription [1], first presented to examine the impact of impurities on superconductivity, is a BCS formalism for an inhomogeneous system and requires *one* diagonalization of the single-particle problem. The purpose of this paper is to examine the limits of applicability of the Anderson approach, as compared to the BdG formalism. We first summarize the two approaches, and then follow with some concrete examples, utilizing surfaces and impurities as sources of inhomogeneities.

We find that the Anderson prescription works very well for surfaces and in some regimes for a single impurity. It breaks down for strong coupling with weak impurity scattering.

For our purposes we adopt a convenient model to describe s-wave superconductivity, the attractive Hubbard Hamiltonian (the results of our study will presumably apply to d-wave or other symmetry states):

$$H - \mu N_e = - \sum_{i,\delta} t_\delta (a_{i+\delta,\sigma}^\dagger a_{i\sigma} + \text{h.c.}) - \sum_{i,\sigma} (\mu - \epsilon_i) n_{i\sigma} - |U| \sum_i n_{i\uparrow} n_{i\downarrow}. \quad (1)$$

Here,  $a_{i\sigma}^\dagger$  ( $a_{i\sigma}$ ) creates (annihilates) an electron with spin  $\sigma$  at site  $i$  and  $n_{i\sigma}$  is the number operator for an electron with spin  $\sigma$  at site  $i$ . The  $t_\delta$  is the hopping rate of

electrons from one site to a neighbouring site (often nearest neighbours only are included, and we will adopt this model here), and  $|U|$  is the attractive coupling strength between electrons on the same site. As usual, this attraction is justified in terms of an electron-phonon coupling, where retardation effects are unimportant, as is the case with many conventional superconductors. The second term includes the chemical potential  $\mu$  and the impurity potential at site  $i$ ,  $\epsilon_i$ . We assume that impurities act to raise or lower single site energy levels. It is worth noting that impurity effects can certainly enter in other ways. For example if an impurity occupies one of the sites, undoubtedly the hopping amplitude to and from that site will also be altered, as will the interaction between two electrons occupying the same orbital on that site. In many studies (see, for example, Ref. [6]), the  $\epsilon_i$  are randomly distributed with some probability distribution, and then the results are averaged, to reflect the fact that we generally have no control over the precise distribution of impurities in the bulk. However, in systems where a single impurity can be added to the surface, for example (see, eg., Ref. [7]), we would want to study this model with only one impurity, at a particular site (in this case, on the surface).

Equation (1) also allows us the freedom to choose periodic boundary conditions (PBC) (to recover well-known results) or ‘open’ boundary conditions (OBC). The latter are natural in a tight-binding context; they require no assumptions about the order parameter, for example. ‘Open’ here simply means that electrons cannot hop beyond the surface. Here again more sophisticated boundary effects could be included — for example, in a real system the hopping integral at the surface will no doubt differ from that in the bulk, but we leave aside these finer points.

The BdG equations are obtained by defining an effective Hamiltonian, with effective potentials [5]. By diagonalizing this effective Hamiltonian through the generalized Bogoliubov-Valatin transformation [5], one arrives at the two BdG equations [8]:

$$E_n u_n(i) = \sum_{i'} A_{ii'} u_n(i') + V_i u_n(i) + \Delta_i v_n(i) \quad (2)$$

$$E_n v_n(i) = - \sum_{i'} A_{ii'} v_n(i') - V_i v_n(i) + \Delta_i^* u_n(i) \quad (3)$$

where

$$A_{ii'} = -t \sum_{\delta} \left( \delta_{i', i-\delta} + \delta_{i', i+\delta} \right) - \delta_{ii'} \left( \mu - \epsilon_i \right). \quad (4)$$

The self-consistent potentials,  $V_i$ , and  $\Delta_i$ , are given by

$$\Delta_i = |U| \sum_n u_n(i) v_n^*(i) (1 - 2f_n) \quad (5)$$

$$V_i = -|U| \sum_n \left[ |u_n(i)|^2 f_n + |v_n(i)|^2 (1 - f_n) \right]. \quad (6)$$

We use the index  $n$  to label the eigenvalues (there are  $2N$  of them), the index  $i$  to label the sites (1 through  $N$ ), and the composite eigenvector is given by  $\begin{pmatrix} u_n \\ v_n \end{pmatrix}$ , of total length  $2N$ . The sums in Eqs. (5,6) are over positive eigenvalues only. The  $f_n$  is the Fermi function, with argument  $\beta E_n$ , where  $\beta \equiv 1/k_B T$ , with  $T$  the temperature. The single site electron density,  $n_i$ , is given, through Eq. (6), by  $V_i = -|U|n_i/2$ .

The equations (5,6) for the effective potentials were determined through a variational principle so that the effective Hamiltonian allows fluctuations in any number of mean fields [5]. As written, there are two possible mean field potentials, the *Hartree potential*,  $V_i$ , and the *pair potential*,  $\Delta_i$ , from which the ground state energy and other properties may be obtained.

An alternate prescription was originally proposed by Anderson [1], whereby one first solves for the eigenvalues and eigenstates of the ‘non-interacting’ problem, i.e.,

$$E_n^0 w_n(i) = \sum_{i'} A_{ii'} w_n(i'). \quad (7)$$

Using the unitary matrix,  $U_{in}$ , for a basis which diagonalizes the single-particle Hamiltonian, one can determine the transformed electron-electron interaction:

$$V_{nm, n' m'} = -|U| \sum_i U_{in}^* U_{im}^* U_{in'} U_{im'}, \quad (8)$$

which now mediates the (generally off-diagonal) electron-electron interaction. The gap and number equations are obtained just as in BCS theory, except that now the label is not the wave vector  $\mathbf{k}$ , but rather some quantum number  $n$ , which simply enumerates the single particle eigenvalues [9]. From the solution, one can obtain the ground state energy and, by transforming back to space coordinates, site-dependent quantities.

The simplest origin of gap inhomogeneity in a superconductor is the surface. The presence of surfaces beyond which electrons are unable to move yields a gap parameter (i.e., pair potential) which can exhibit a variety of

behaviour near the surface. Traditionally in Ginzburg-Landau treatments the gap function is given a priori a boundary condition [5]; here the behaviour near a boundary (or impurity) is a derived quantity, i.e. as the solution to the BdG (or Anderson) equations.

The advantage (for the Anderson approach) of examining the impact of surfaces on the gap parameter is that an analytical solution exists for a simple tight-binding model [10]. The eigenstates for a chain [11] of length  $N$ , with lattice spacing  $a$  and nearest-neighbour hopping  $t$ , are

$$a_{k\sigma} = \sqrt{\frac{2}{N+1}} \sum_i \sin(kR_i) a_{i\sigma}, \quad (9)$$

and the eigenenergies are

$$E_k^{(0)} = -2t \cos(ka), \quad ka = \frac{\pi n}{N+1}, \quad (10)$$

where  $n = 1, 2, \dots, N$ . We use these analytical results in the Anderson approach (making it not significantly more difficult than BCS theory), while in the BdG approach these analytical solutions are not particularly helpful.

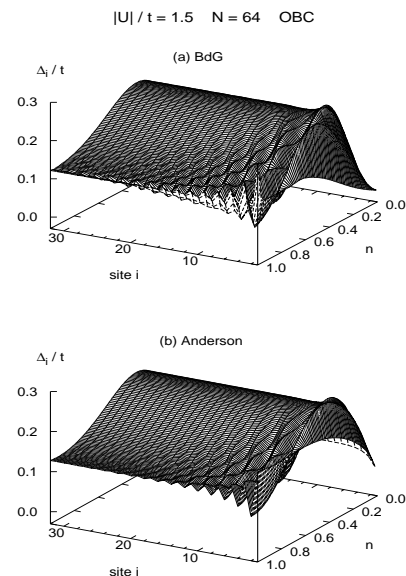


FIG. 1. Gap parameter  $\Delta_i$  as a function of site number  $i$  and electron density  $n$ , for  $N = 64$  with OBC and  $|U| = 1.5t$ . The BdG and Anderson results are shown in (a) and (b), respectively.

In Fig. 1 we show the gap parameter  $\Delta_i$  as a function of site number  $i$ , for electron density  $n$  ranging from half-filling to zero. The chain length is 64 sites, and we have used OBC and the coupling strength  $|U| = 1.5t$ . Here  $\Delta_i$  is shown for half the chain length (from  $i = 1$  to 32): the gap parameter is symmetric about the middle. In Fig. 1(a) we plot the result from the BdG equations,

while in Fig. 1(b) we show the corresponding results from the Anderson prescription. The first thing to note is that in either case the behaviour near the surface is markedly different as a function of electron density. At half-filling the gap parameter actually peaks at the surface, with several ‘Friedel-like’ oscillations ensuing towards the center of the sample, while at low fillings the gap parameter is much smoother by comparison. A comparison of the two figures shows quantitative differences, but overall, qualitatively they are very similar. It is evident that the Anderson prescription captures the essence of the BdG results remarkably well.

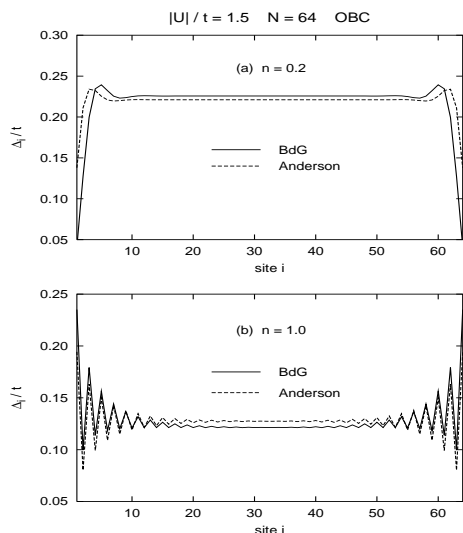


FIG. 2. Cross sections of  $\Delta_i$  shown in Fig. 1 at density (a)  $n = 0.2$  and (b)  $n = 1.0$ . The BdG and Anderson results are now plotted together, in solid and dashed lines, respectively. It can be clearly seen that the Anderson prescription reproduces the BdG results very well.

The accuracy of the Anderson results can be seen more closely in Fig. 2, where the cross sections of  $\Delta_i$  versus  $i$  in Fig. 1 for (a)  $n = 0.2$  and (b)  $n = 1.0$  are shown. It is clear that the essential features of the BdG results are reproduced in the Anderson approach.

To examine the effect of impurities, we show in Fig. 3  $\Delta_i$  as a function of  $i$ , for  $N = 32$  with an impurity at the central site with varying energy (both negative and positive). We have used PBC and an intermediate coupling strength,  $|U| = 2t$ , at electron density  $n = 0.9$ . We have intentionally stayed away from half-filling, at which the ground state is not a superconducting state, but a charge density wave. One may recall that with periodic boundary conditions and with no impurities, the ground state for the attractive Hubbard model at half-filling is doubly degenerate: both superconducting and charge density wave solutions coexist at this point. However, the presence of an impurity tilts the balance in favour of the

charge density wave, and the BdG equations converge to a solution in which the pair potential,  $\Delta_i$ , is identically zero at all sites. The Hartree potential,  $V_i$ , on the other hand, oscillates as a function of site position. The Anderson prescription is unable to reproduce this (correct) feature at half filling, and gives a superconducting solution with nonzero gap parameters. Also if the self-consistency of the Hartree potential is neglected in the BdG equations, this physics is missed, and the ensuing BdG result is similar to the Anderson solution.

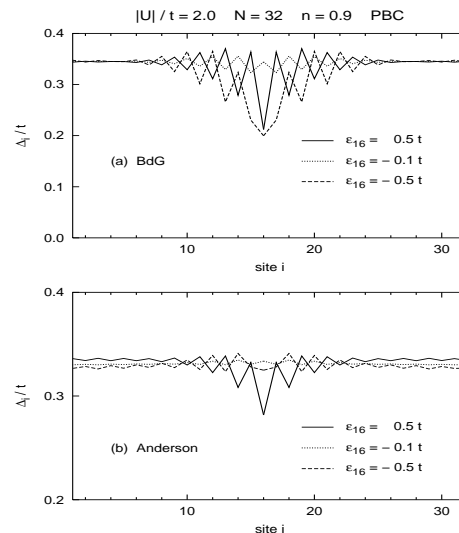


FIG. 3. Gap parameter  $\Delta_i$  as a function of site number  $i$ , for a chain of  $N = 32$  with PBC and an impurity at site 16 with varying potential energy, from the (a) BdG and (b) Anderson equations. Note that in (b) the scale of the gap is twice the scale in (a).

Returning to Fig. 3 we have plotted the BdG results in Fig. 3(a), while in Fig. 3(b) we show the results from the Anderson equations. The gap is suppressed at the site with a positive impurity potential (as is the site density  $n_i$ ) and exhibits ‘Friedel-like’ oscillations around it. The Anderson prescription captures this behaviour qualitatively, while it tends to underestimate the amplitudes of the oscillations (compare the solid curves in Fig. 3(a) and (b) for  $\epsilon_{16} = 0.5t$ , and note the magnified scale in the latter graph). The Anderson results become better for stronger impurity potentials and for electron density  $n$  further away from half filling. For a negative impurity potential, when the potential strength is very weak,  $\Delta_i$  (and  $n_i$ ) has a peak at the impurity site, as can be seen in Fig. 3(a) for  $\epsilon_{16} = -0.1t$  (the dotted curve). Though smaller in scale, the Anderson result in Fig. 3(b) has similar behaviour. As the potential strength increases, however, an attractive impurity tends to break the pairing, and suppresses the gap not only at the impurity site but also at surrounding sites (see the dashed curve for

$\epsilon_{16} = -0.5t$  in Fig. 3(a)). In such cases, the Anderson method overestimates the gap parameter around the impurity site. This can be seen in Fig. 3(b), where the gap has the correct oscillating pattern, but with much smaller amplitudes.

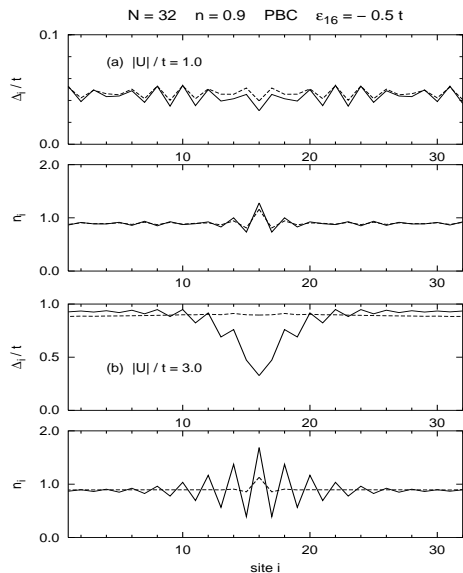


FIG. 4. The  $\Delta_i$  as a function of  $i$ , for a chain of  $N = 32$  with PBC and  $\epsilon_{16} = -0.5t$ , for (a)  $|U| = 1t$  and (a)  $|U| = 3t$ . The BdG and Anderson results are plotted in solid and dashed curves, respectively.

We study the attractive impurity case further in Fig. 4, where we show  $\Delta_i$  and  $n_i$  versus  $i$  for  $N = 32$  with PBC and  $\epsilon_{16} = -0.5t$ , for (a)  $|U| = 1t$  and (b)  $|U| = 3t$ . When the coupling is weaker than or comparable to the impurity potential, the Anderson approach captures the main features of the gap parameter around the impurity. This is the case for  $|U| = 1t$  in Fig. 4(a), and indeed the Anderson results show excellent agreement with the BdG results. As the coupling becomes stronger compared to the impurity potential, the impact of the impurity becomes more drastic, even with relatively weak strength. The gap is more suppressed around the impurity, and the density distribution exhibits ‘Friedel-like’ oscillations more enhanced. This can be seen for  $|U| = 3t$  in Fig. 4(b) (solid curves). On the other hand, the Anderson method yields a gap parameter that is more uniform as a function of site position, and does not reproduce the correct oscillations in the site densities.

In conclusion, we have formulated the BdG equations for a tight-binding model with an on-site attractive interaction. We have retained the self-consistent Hartree potential in the BdG equations, and found that a single impurity breaks the superconducting/charge density wave degeneracy which would otherwise exist at half-filling in this model. We have also formulated the prescription set

out by Anderson, without impurity-averaging, and found good qualitative agreement with the BdG results.

To our knowledge, the spatial dependence of the order parameter and the electron density has not been previously explored in detail within the Anderson prescription. We have found, somewhat to our surprise, good agreement with results from the BdG formalism, for surfaces and single impurities (aside from the weak scattering limit). Throughout this study, it is important to note that in the vicinity of surfaces or impurities, ‘‘charge ordered’’ states and superconductivity in general coexist (at the mean field level). In future work we will examine various correlation functions and the local density of states, the latter of which has been [7] and will continue to be measured using scanning tunneling microscopy.

*Acknowledgements* We thank Jorge Hirsch for suggesting the weak impurity potential regime as one in which the Anderson prescription should break down. We also thank Kamran Kaveh for stimulating discussions. Calculations were performed on the 64-node SGI parallel processor at the University of Alberta. This research was supported by the Avadh Bhatia Fellowship and by the Natural Sciences and Engineering Research Council of Canada and the Canadian Institute for Advanced Research.

- 
- [1] P. W. Anderson, J. Phys. Chem. Solids **11**, 26 (1959).
  - [2] A.A. Abrikosov and L.P. Gor’kov, Sov. Phys. JETP **8**, 1090 (1959).
  - [3] See G.P. Collins, in *Physics Today, Search and Discovery*, p.17, 1993, and M.F. Crommie, C.P. Lutz, and D.M. Eigler, Science **262**, 218 (1993).
  - [4] *Quasiclassical Methods in Superconductivity and Superfluidity*, edited by D. Rainer and J.A. Sauls, 1996.
  - [5] P. G. de Gennes, *Superconductivity of Metals and Alloys* (W.A. Benjamin, Inc. New York, 1966).
  - [6] A. Ghosal, M. Randeria, and N. Trivedi, Phys. Rev. Lett. **81**, 3940 (1998).
  - [7] E.W. Hudson, S.H. Pan, A.K. Gupta, K.-W. Ng, and J.C. Davis, Science **285**, 88 (1999).
  - [8] For a tight-binding formulation of the BdG equations, see J.E. Hirsch, Physica C **194** 119 (1992). Note that he excluded the Hartree-Fock potential.
  - [9] K. Tanaka and F. Marsiglio, Phys. Lett. A **265**, 133 (2000).
  - [10] We thank Stuart Trugman for alerting us to this analytical solution.
  - [11] In this work we use one dimensional chains, partly because real space results are more easily illustrated, and partly because for the attractive Hubbard model, dimensionality should not play a very important role (at the mean field level), so that results presented here are generally applicable to two and three dimensions.